

Label-Free Imaging of Lipophilic Bioactive Molecules during Lipid Digestion by Multiplex Coherent Anti-Stokes Raman Scattering Microspectroscopy

James P. R. Day,[†] Gianluca Rago,[†] Katrin F. Domke,[†] Krassimir P. Velikov,[‡] and Mischa Bonn^{*,†}

FOM Institute for Atomic and Molecular Physics (AMOLF), Science Park 104, 1098 XG Amsterdam, The Netherlands, and Unilever R&D Vlaardingen, Olivier Noortlaan 120, NL-3133 AT Vlaardingen, The Netherlands

Received March 11, 2010; E-mail: bonn@amolf.nl

Abstract: The digestion and absorption of lipophilic, bioactive molecules such as lipids, physiologically active nutrients (nutraceuticals), and drugs play a crucial role in human development and health. These molecules are often delivered in lipid droplets. Currently, the kinetics of digestion of these lipid droplets is followed by in vitro models that simulate gastrointestinal conditions, while phase changes within the lipid droplets are observed by light or electron microscopy. However real-time, spatially resolved information about the local chemical composition and phase behavior inside the oil droplet is not accessible from these approaches. This information is essential as the surface and phase behavior determine the local distribution of molecules in the oil droplets and thus may influence the rate of uptake, for example, by impairing the effective transfer of bioactive molecules to intestinal cells. We demonstrate the capability of multiplex coherent anti-Stokes Raman scattering (CARS) microspectroscopy to image the digestion process non-invasively, with submicrometer resolution, millimolar sensitivity, and without the need for labeling. The lipolysis of glyceryl trioleate emulsion droplets by porcine pancreatic lipase is imaged, and the undigested oil and the crystalline lipolytic products are distinguished by their different vibrational signatures. The digestion of droplets containing the phytosterol analogue ergosterol is also probed, and the crystals are observed to dissolve into the lipolytic products. The lipophilic drug progesterone and Vitamin D₃ are dissolved in glyceryl trioctanoate emulsion droplets, and the local concentration is mapped with millimolar sensitivity. The bioactive molecules are observed to concentrate within the droplets as the oil is hydrolyzed. This observation is ascribed to the low solubility of these molecules in the lipolytic products for this system. Neither the type of bioactive molecule nor the initial radius of the emulsion droplet had a large effect upon the rate of digestion under these conditions; lipolysis of the triglyceride by pancreatic lipase appears insensitive to the type of bioactive molecule in solution. These findings shed important new light on lipid digestion and open new possibilities for the chemical visualization of lipid digestion and phase changes in lipid droplets containing bioactive molecules, which in combination with other existing techniques will provide a full picture of this complex physicochemical process.

Introduction

The digestion and absorption of lipophilic, bioactive molecules such as lipid nutrients, oil-soluble vitamins, and nutraceuticals such as cholesterol-lowering food additives (e.g., phytosterols) play vital roles in human growth, development, and well-being.¹ Furthermore, the continuing search for effective drugs often leads to highly potent, but poorly water-soluble candidates, particularly since the advent of combinatorial chemistry as a major synthetic technique.² These bioactive molecules are introduced to the body within lipid excipients, and lipid digestion is now recognized as a critical factor in their delivery to the circulatory systems of the body. However,

digestion is a complex process that has not yet been fully understood.^{3,4} This gap in our knowledge can be traced to the challenges associated with observing non-invasively and in real-time the behavior of both the bioactive molecule and the lipid excipient during digestion: techniques that allow us to do so would certainly further our understanding of these complex, important processes. In this paper, we introduce multiplex coherent anti-Stokes Raman scattering (CARS) microspectroscopy as a powerful and versatile tool to image not only the bioactive molecule and lipid excipient during digestion but also the lipolytic products of digestion, without the need for labeling. We follow this process non-invasively and with submicrometer spatial resolution. It is demonstrated that multiplex CARS microspectroscopy is able to quantify the concentration of the

[†] FOM Institute for Atomic and Molecular Physics.

[‡] Unilever R&D Vlaardingen.

(1) *Handbook of Nutraceuticals and Functional Foods*, 2nd ed.; Wildman, R. E. C., Ed.; CRC Press: Boca Raton, FL, 2007.
 (2) Porter, C. J. H.; Trevaskis, N. L.; Charman, W. N. *Nat. Rev. Drug Discovery* **2007**, *6*, 231–248.

(3) McClements, D. J.; Decker, E. A.; Park, Y. *Crit. Rev. Food Sci. Nutr.* **2009**, *49*, 48–67.

(4) Porter, C. J. H.; Pouton, C. W.; Cuine, J. F.; Charman, W. N. *Adv. Drug Delivery Rev.* **2008**, *60*, 673–691.

bioactive molecule in the excipient during digestion with millimolar sensitivity. This technique offers the unparalleled opportunity to actually observe and quantify the evolution of a digesting system and hence to obtain information about the mechanisms by which the uptake of bioactive molecules occurs.

Lipid digestion is a dynamic and complex process, during which the lipid undergoes several changes in phase.⁵ After ingestion, a liquid triacylglyceride oil is partially hydrolyzed in the stomach by gastric lipase enzyme into diglycerides, monoglycerides, and fatty acids and churned into a coarse, polydisperse emulsion by the mechanical action of the stomach. This emulsion is passed into the small intestine and further hydrolyzed by pancreatic lipase. The lipolytic products (diglycerides, monoglycerides, and fatty acids) have only a limited solubility in the aqueous luminal fluid of the gastrointestinal (GI) tract and form liquid crystalline phases on the surface of the emulsion droplet.^{6,7} These liquid crystal phases are dispersed by bile into dietary mixed micelles (DMMs) and vesicles which are soluble in the luminal fluid, and these colloidal products are ultimately transported to and absorbed by the enterocyte cells that line the gut wall.⁸

Bioactive molecules are most efficiently transported and absorbed when the molecule remains in solution throughout these digestion and uptake stages.⁹ The partitioning of bioactive molecules among the various phases has been observed indirectly by removing and analyzing aliquots from model digestion experiments, but this approach destroys any information about the spatial distribution of the bioactive molecule within a phase.⁴ Electron paramagnetic resonance spectroscopy has been used to follow the partitioning of a model drug in real time, but this technique is not spatially resolved and requires paramagnetic labeling.¹⁰ The different phases of the lipolytic products have been observed directly by freeze-fracture electron microscopy, but this approach cannot distinguish different chemical species and is inherently destructive.^{6,7,11} Ideally, one would want to obtain both spatially and chemically resolved information about the behavior of both the bioactive molecule and the lipolytic product phases in order to investigate the mechanisms by which the bioactive molecule is transported and absorbed by the body. This information is essential as surface and phase changes determine the local distribution of molecules in the oil droplets and may affect the rate of digestion and influence the effective transfer of bioactive molecules into DMMs and the intestinal cells.³ Here we will show that multiplex CARS microspectroscopy is well-suited to obtain precisely this information.

Multiplex CARS microspectroscopy is a chemically specific, label-free, non-invasive form of hyperspectral imaging with submicrometer spatial resolution in which the contrast in an image is derived from molecular vibrations.^{12–14} As such, one is able to identify different chemical species directly due to the

unique vibrational fingerprints shown by different molecules. It has proven to be an invaluable tool to investigate problems across a range of scientific disciplines.^{15–18} Recent efforts to extend the spectral bandwidth of multiplex CARS using super-continuum sources^{19,20} or pulse shaping^{21,22} further extend the applicability of this technique. Raman microspectroscopy and single-frequency CARS microscopy have also been used extensively in cell and tissue biology to acquire images based on vibrational contrast exhibited by different chemical species.^{23–30}

In this contribution, we first investigate the digestion of a triacylglyceride oil droplet by pancreatic lipase in the absence of any additives, and we demonstrate the capability of CARS microspectroscopy to discriminate between the undigested oil and lipolytic products based on their vibrational signatures. We also map the evolution of the digestion process in order to specify the locations at which the lipolytic products are generated. We then observe the behavior of undissolved ergosterol crystals in a saturated solution during lipolysis. Ergosterol is a chemical analogue of phytosterols and cholesterol. Phytosterols have drawn considerable attention in recent years due to their ability to lower blood cholesterol levels when incorporated into foodstuffs such as margarine.^{31–34} However, detailed, non-invasive, spatially resolved information about the behavior of these additives during the digestion of their carrier phase in the GI tract and their effect on the digestion process has hitherto been inaccessible. Here we demonstrate the potential of CARS microspectroscopy to identify ergosterol crystals within an oil droplet and to follow their solvation by lipolytic products. Finally, we follow the digestion of oil droplets in which the lipophilic drugs progesterone or Vitamin D₃ have been dissolved. Drug delivery systems range from simple formulations in which the drug is dissolved or suspended in the lipid excipient to more complex self-emulsifying and self-micro-emulsifying formulations.⁴ In recent years, it has been realized that these excipients are not merely passive delivery agents for the drug but actively influence the bioavailability and efficacy.

- (5) Mu, H. L.; Hoy, C.-E. *Prog. Lipid Res.* **2004**, *43*, 105–133.
- (6) Rigler, M. W.; Honkanen, R. E.; Patton, J. S. *J. Lipid Res.* **1986**, *27*, 836–857.
- (7) Rigler, M. W.; Patton, J. S. *Biochim. Biophys. Acta* **1983**, *751*, 444–454.
- (8) Ros, E. *Atherosclerosis* **2000**, *151*, 357–379.
- (9) MacGregor, K. J.; Embleton, J. K.; Lacy, J. E.; Perry, E. A.; Solomon, L. J.; Seager, H.; Pouton, C. W. *Adv. Drug Delivery Rev.* **1997**, *25*, 33–46.
- (10) Rube, A.; Klein, S.; Mader, K. *Pharm. Res.* **2006**, *23*, 2024–2029.
- (11) Mazur, A. W.; Burns, J. L.; Hiler, G. D.; Spontak, R. J. *J. Phys. Chem.* **1993**, *97*, 11344–11349.
- (12) Volkmer, A. *J. Phys. D* **2005**, *38*, R59–R81.
- (13) Muller, M.; Zumbusch, A. *ChemPhysChem* **2007**, *8*, 2156–2170.
- (14) Evans, C. L.; Xie, X. S. *Annu. Rev. Anal. Chem.* **2008**, *1*, 883–909.

- (15) Rinia, H. A.; Burger, K. N. J.; Bonn, M.; Muller, M. *Biophys. J.* **2008**, *95*, 4908–4914.
- (16) Kox, M. H. F.; Domke, K. F.; Day, J. P. R.; Rago, G.; Stavitski, E.; Bonn, M.; Weckhuysen, B. M. *Angew. Chem., Int. Ed.* **2009**, *48*, 8990–8994.
- (17) Koster, J.; Schlucker, S. *J. Raman Spectrosc.* **2008**, *39*, 942–952.
- (18) Camp, C. H.; Yegnanarayanan, S.; Eftekhari, A. A.; Sridhar, H.; Adibi, A. *Opt. Express* **2009**, *17*, 22879–22889.
- (19) Kano, H.; Hamaguchi, H. *Anal. Chem.* **2007**, *79*, 8967–8973.
- (20) Lee, Y. L.; Liu, Y.; Cicerone, M. T. *Opt. Lett.* **2007**, *32*, 3370–3372.
- (21) Sung, J.; Chen, B.-C.; Lim, S.-H. *J. Raman Spectrosc.* [Online early access]. DOI: 10.1002/jrs.2647. Published Online: March 25, 2010.
- (22) Lee, Y. J.; Cicerone, M. T. *Opt. Express* **2009**, *17*, 123–135.
- (23) Lee, B.; Zhu, J.; Wolins, N. E.; Cheng, J.-X.; Buhman, K. K. *Biochim. Biophys. Acta* **2009**, *1791*, 1173–1180.
- (24) Hellerer, T.; Axang, C.; Brackmann, C.; Hillertz, P.; Pilon, M.; Enejder, A. *Proc. Natl. Acad. Sci. U.S.A.* **2007**, *104*, 14658–14663.
- (25) Balu, M.; Liu, G.; Chen, Z.; Tromberg, B. J.; Potma, E. O. *Opt. Express* **2010**, *18*, 2380–2388.
- (26) Nan, X. L.; Potma, E. O.; Xie, X. S. *Biophys. J.* **2006**, *91*, 728–735.
- (27) Le, T. T.; Duren, H. M.; Slipchenko, M. N.; Hu, C. D.; Cheng, J.-X. *J. Lipid Res.* **2010**, *51*, 672–677.
- (28) van Manen, H.-J.; Lenferink, A.; Otto, C. *Anal. Chem.* **2008**, *80*, 9576–9582.
- (29) Matthaus, C.; Chernenko, T.; Newmark, J. A.; Warner, C. M.; Diem, M. *Biophys. J.* **2007**, *93*, 668–673.
- (30) Pully, V. V.; Otto, C. *J. Raman Spectrosc.* **2009**, *40*, 473–475.
- (31) Mehtiev, A. R.; Misharin, A. Y. *Biochemistry (Moscow)* **2008**, *2*, 1–17.
- (32) Ostlund, R. E. *Curr. Opin. Lipidol.* **2004**, *15*, 37–41.
- (33) Rozner, S.; Garti, N. *Colloids Surf., A* **2006**, *282–283*, 435–456.
- (34) Trautwein, E. A.; Duchateau, G. S. M. J. E.; Lin, Y.; Mel'nikov, S. M.; Molhuizen, H. O. F.; Ntanos, F. Y. *Eur. J. Lipid Sci. Technol.* **2003**, *105*, 171–185.

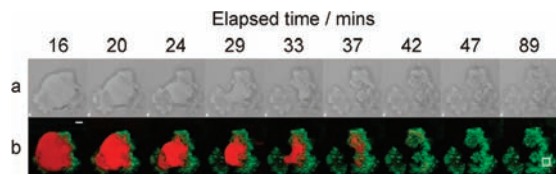


Figure 1. Time-resolved images of the digestion of a glyceryl trioleate droplet by porcine pancreatic lipase. (a) Bright-field microscopy images; (b) false-color images obtained by CARS microspectroscopy of glyceryl trioleate (red) and lipolytic products (green). The brightness of each pixel corresponds to linear fit coefficients from individual spectra, as discussed in the text. Scale bar = 5 μm , pixel step size = 1 μm , 41×41 pixels, measurement time per image = 35 s. Enzyme concentration = 1.5 mg mL^{-1} . White square: area used to generate representative spectrum of the lipolytic products.

The excipient is known to affect numerous aspects of drug uptake, including drug solubilization in the aqueous luminal fluid of the gastrointestinal (GI) tract, passive and active transport through cell membranes, intracellular processing and metabolism, and delivery of the drug to specific sites within the cell.³⁵ However, the mechanisms by which the excipient enhances drug action are not fully understood and are evidently of interest if we wish to create the most efficient and effective drug formulations. Progesterone is used to supplement the body's natural levels during in vitro fertilization and hormone therapy, but the drug exhibits low oral bioavailability and is often administered in oil.³⁶ The fat-soluble Vitamin D₃ is also often included in nutritional supplements to boost natural levels in the body. The partitioning behavior of both of these drugs during digestion has been followed in vitro and in vivo by HPLC,³⁷ but this approach lacks spatially resolved information. Here we obtain quantitative maps of the drug concentration within an oil droplet during digestion as a function of time.

Results and Discussion

Digestion of Glyceryl Trioleate. In the first set of experiments, we used glyceryl trioleate as the triglyceride oil phase. This triglyceride comprises three oleic acid chains. Oleic acid is a C₁₈ monounsaturated fatty acid and the major fatty acid constituent of olive oil. Bright-field microscopy images of the digestion of an oil droplet over the course of 90 min are shown in Figure 1a. In the first image of the sequence (16 min after digestion was initiated), the enzyme has begun to digest the liquid oil, as evinced by the presence of a crystalline phase on the lower left and the right side of the droplet.³⁸ During lipolysis, each molecule of triacylglyceride is ultimately hydrolyzed into two molecules of fatty acid and one molecule of monoglyceride. The phase behavior of this multicomponent mixture is complex and depends, among others, upon the nature of the hydrocarbon chain and the local composition.³⁹ By the final image (after 89 min), all of the oil has been hydrolyzed and only the crystalline lipolytic products remain. No further evolution—either spectrally or spatially—was observed. During the hydrolyzation process, we acquired hyperspectral CARS images of the oil droplet, and analyzed each raw CARS spectrum by the maximum entropy method to retrieve the $\text{Im}[\chi^{(3)}]$ spectrum, as described in the

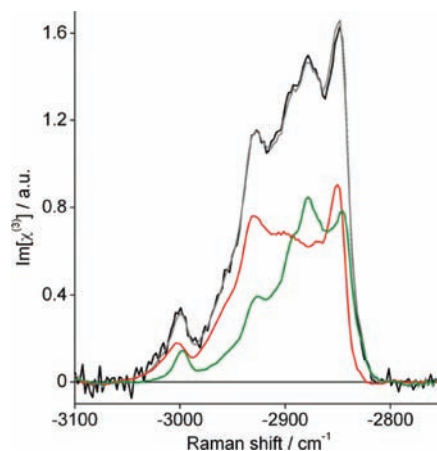


Figure 2. $\text{Im}[\chi^{(3)}]$ spectra of undigested glyceryl trioleate (red), lipolytic products (green), and an individual pixel within a partially digested drop (black). A linear combination fit of the green and red spectra to the black spectrum is also shown (gray).

Experimental Section. $\text{Im}[\chi^{(3)}]$ spectral intensities are proportional to the number of moieties in the laser focus that vibrate at that frequency and are directly comparable to Raman spectra. In Figure 2, a spectrum of undigested glyceryl trioleate is shown in red. Spectra from a $5 \times 5 \mu\text{m}$ region (within the white square) in the lower right of the final image were averaged to generate a representative spectrum of the lipolytic products. This spectrum is shown in Figure 2 in green. The spectrum of the undigested oil is typical of an unsaturated hydrocarbon; in particular, the ratio of the antisymmetric and symmetric methylene stretches at -2892 and -2850 cm^{-1} indicates that the oil is liquid.⁴⁰ In contrast, in the spectrum of the lipolytic products, this ratio is greater and the peaks are shifted to the lower frequencies of -2878 and -2845 cm^{-1} . These changes are indicative of a hydrocarbon chain in a more ordered environment, as expected for a crystalline phase.⁴¹ A typical spectrum from an individual pixel within the partially digested drop is also shown in Figure 2 in black. This spectrum contains contributions from both the liquid oil and the crystalline lipolytic products in proportion to their local concentration within the pixel. We therefore treat this spectrum as a linear combination of the spectra of the undigested oil and the lipolytic products to generate the fit shown in Figure 2 in gray.⁴² We then plot the coefficients of the fit at each pixel to generate the false-color images shown in Figure 1b. These coefficients are proportional to the concentration; brighter colors in the image correspond to higher concentrations.

The bright-field and CARS images correlate well. This correlation confirms that the vibrational signatures of the undigested oil and the lipolytic products are sufficiently distinct to discriminate these phases by multiplex CARS microspectroscopy. However, the CARS images display enhanced contrast compared to the bright-field images. Furthermore, one can distinguish regions of the image in which both phases coexist. In both sets of images, the lipolytic products are seen around the edge of the droplet, as expected. The enzyme is only soluble in the aqueous phase, so it can only hydrolyze the triglyceride at the oil–water interface, and thus the lipolytic products are formed exclusively at this interface. Three other equivalent

(35) Porter, C. J. H.; Wasan, K. M.; Constantinides, P. *Adv. Drug Delivery Rev.* **2008**, *60*, 615–616.

(36) Tuleu, C.; Newton, M. R., Jr.; Euler, D.; Saklatvala, R.; Clarke, A.; Booth, S. *J. Pharm. Sci.* **2004**, *93*, 1495–1502.

(37) Dahan, A.; Hoffman, A. *Pharm. Res.* **2006**, *23*, 2165–2174.

(38) Patton, J. S.; Carey, M. C. *Science* **1979**, *204*, 145–148.

(39) Kossena, G. A.; Charman, W. N.; Boyd, B. J.; Dunstan, D. E.; Porter, C. J. H. *J. Pharm. Sci.* **2004**, *93*, 332–348.

(40) Snyder, R. G.; Strauss, H. L.; Elliger, C. A. *J. Phys. Chem.* **1982**, *86*, 5145–5150.

(41) Lee, C.; Bain, C. D. *Biochim. Biophys. Acta* **2005**, *1711*, 59–71.

(42) Bro, R.; DeJong, S. *J. Chemom.* **1997**, *11*, 393–401.

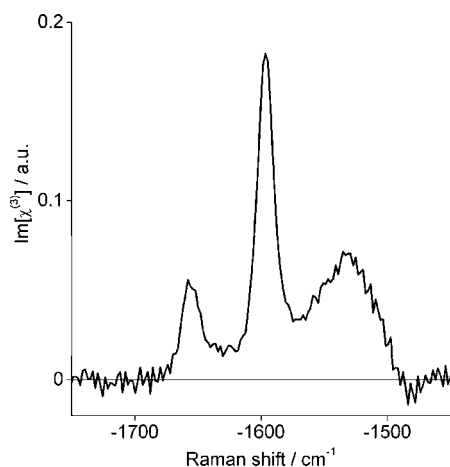


Figure 3. $\text{Im}[\chi^{(3)}]$ spectrum of 0.2 M ergosterol dissolved in CCl_4 . Note that the broad band centered at -1530 cm^{-1} arises from the CCl_4 solvent.

samples were also investigated and displayed comparable behavior (data not shown).

Solvation of Ergosterol by the Lipolytic Products of Digestion. Bright-field microscopy images of the digestion of two different oil droplets containing 10 wt % ergosterol over 45 and 90 min, respectively, are shown in Figures 4a and 5a. Ergosterol is above its solubility limit at this concentration, and crystals are visible in the first image of each sequence on the left-hand side of the droplet in Figure 4 and toward the top of the droplet in Figure 5. It is not possible to distinguish between ergosterol crystals and the lipolytic products by bright-field microscopy; both species are expected to appear as crystals. However, CARS microspectroscopy achieves contrast through differences in the vibrational signatures of chemicals, so different species can be identified and the distribution of ergosterol within the droplet can still be determined throughout the lipolysis reaction.

For this experiment, we acquired CARS spectra centered at a Raman shift of -1550 cm^{-1} . The Raman scattering cross section, and hence the CARS response, of hydrocarbons is lower in this frequency regime than in the C–H stretching region, but the three components can be more readily distinguished here. The differences in the spectra in the C–H stretching region of the undigested oil and lipolytic products are mirrored in the C–C stretch and C–H bending modes in the range from -1400 to -1500 cm^{-1} ; moreover, ergosterol contains two conjugated C=C bonds which manifest as a strong peak at -1600 cm^{-1} .⁴³ A spectrum of 0.2 M ergosterol in CCl_4 is shown in Figure 3. The broad band centered at -1530 cm^{-1} arises from the CCl_4 solvent. False-color CARS images of the digestion of the oil droplets in Figures 4a and 5a are shown in Figures 4b and 5b, respectively.

We observe that the phase behavior of the droplets in Figures 4 and 5 is different, both from each other and from the droplet in Figure 1. In Figure 4, a large amount of lipolytic products is formed, which remains localized on the surface of the oil droplet, whereas in Figure 5, very little lipolytic product is visible. These observations are mirrored in the bright-field images: no crystalline phase is evident in Figure 5a. It appears that the presence of ergosterol in the oil droplets affects the phase behavior during

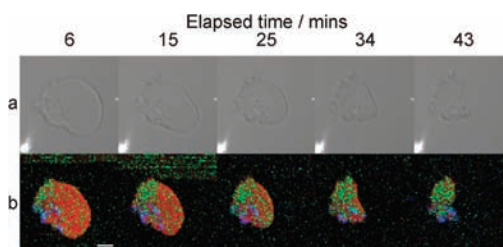


Figure 4. Time-resolved images of the digestion of a glyceryl trioleate droplet containing ergosterol by porcine pancreatic lipase. (a) Bright-field microscopy images; (b) false-color images obtained by CARS microspectroscopy of undigested glyceryl trioleate (red), lipolytic product (green), and ergosterol (blue). The brightness of each pixel corresponds to linear fit coefficients from individual spectra, as discussed in the text. Scale bar = $5 \mu\text{m}$, pixel step size = $0.5 \mu\text{m}$, 61×61 pixels, measurement time per image = 150 s. Enzyme concentration = 1.5 mg mL^{-1} . Note that the lipolytic product remains at the surface of the droplet.

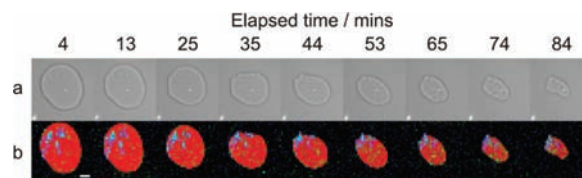


Figure 5. Time-resolved images of the digestion of a glyceryl trioleate droplet containing ergosterol by porcine pancreatic lipase. (a) Bright-field microscopy images; (b) false-color images obtained by CARS microspectroscopy of undigested glyceryl trioleate (red), lipolytic product (green), and ergosterol (blue). The brightness of each pixel corresponds to linear fit coefficients from individual spectra, as discussed in the text. Scale bar = $5 \mu\text{m}$, pixel step size = $1 \mu\text{m}$, 31×31 pixels, measurement time per image = 40 s. Enzyme concentration = 1.5 mg mL^{-1} . Note that, as opposed to the results of Figure 4, the lipolytic product is largely invisible, demonstrating that it readily dissolves into the aqueous phase.

digestion; that is, not only does the lipid excipient actively affect the bioavailability of the sterol, but high local concentrations of the sterol will also reciprocally affect the digestion of the lipid.

During digestion, the ergosterol crystals are reduced in size in both droplets. Ergosterol possesses no ester groups, so the lipase does not act on the crystals directly: ergosterol is dissolving into the lipolytic product. This dissolution is a crucial stage in the uptake of sterols by the body. Sterols that remain within a lipid emulsion cannot be absorbed by enterocytes. The triglycerides must be digested first so that the sterol can dissolve into the dietary mixed micelles.⁴⁴ The observed differences in the digestion of nominally identical lipid droplets of Figures 4 and 5 may be traced to the different local concentrations of sterols, resulting in more efficient dissolution of the lipolytic products in Figure 5.

Quantitative Mapping of the Concentration of Progesterone or Vitamin D₃ in Emulsion Droplets during Digestion. For this study, we used glyceryl trioleate as the oil phase. Glyceryl trioleate is a medium chain-length (C_8) saturated triglyceride that is spectrally transparent between -1550 and -1700 cm^{-1} , a region of the spectrum where unique peaks from the drugs appear. In Figure 6, we present a spectrum of a 95 mM solution of progesterone (red) and a spectrum of a 75 mM solution of Vitamin D₃ (black) in glyceryl trioleate. The peak at -1735 cm^{-1} in each spectrum is the carbonyl stretch from the ester species in glyceryl trioleate. The peak at -1643 cm^{-1} arises from the C=C stretching vibration of the three conjugated

(43) De Gussem, K.; Vandenabeele, P.; Verbeke, A.; Moens, L. *Spectrochim. Acta, Part A* **2005**, *61*, 2896–2908.

(44) Young, S. C.; Hui, D. Y. *Biochem. J.* **1999**, *339*, 615–620.

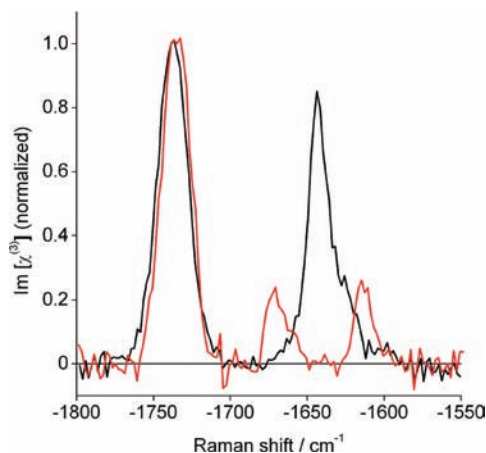


Figure 6. Normalized $\text{Im}[\chi^{(3)}]$ spectra of a 95 mM solution of progesterone (red) and 75 mM solution of Vitamin D₃ (black) in glyceryl trioctanoate. Acquisition time = 5 s.

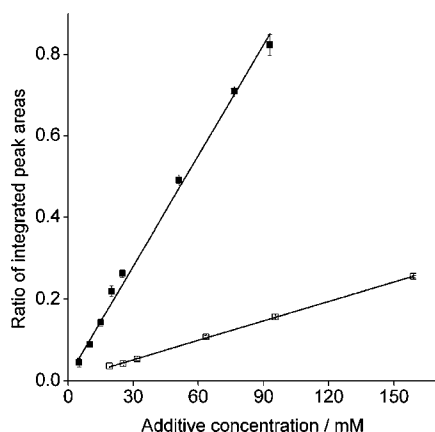


Figure 7. Calibration plots of the ratio between the integrated area of the -1643 cm^{-1} Vitamin D₃ peak and the -1735 cm^{-1} glyceryl trioctanoate peak plotted as a function of Vitamin D₃ concentration (■). The ratio between the integrated area of the -1613 cm^{-1} progesterone peak and the -1735 cm^{-1} glyceryl trioctanoate peak plotted as a function of progesterone concentration (□).

unsaturated bonds in Vitamin D₃. The peaks at -1613 and -1670 cm^{-1} arise from the C=C stretching and C=O stretching vibrations in the α,β -unsaturated carbonyl group of progesterone.⁴⁵

The peak from the oil phase at -1735 cm^{-1} acts as an internal standard; consequently, the ratio between the drug peaks and the oil peak can be used in conjunction with a calibration plot to determine directly the *local* drug concentration within an oil droplet. In theory, this approach is also applicable to determine the concentration of dissolved ergosterol in Figures 4 and 5; however, the signal from the sterol is weaker than the signal from these drugs. Solutions of known concentration of progesterone or Vitamin D₃ in glyceryl trioctanoate were prepared and their CARS spectra measured. In Figure 7, we show the resulting calibration plots of the ratio of the integrated area of the drug and oil peaks as a function of concentration for both progesterone and Vitamin D₃. Under these experimental conditions, the concentration of Vitamin D₃ can be readily determined down to a concentration of ~ 5 mM and the concentration of progesterone can be determined down to ~ 20 mM.

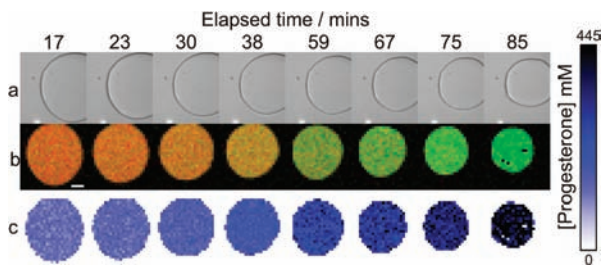


Figure 8. Time-resolved images of the digestion by porcine pancreatic lipase of a glyceryl trioctanoate droplet containing progesterone at an initial concentration of 95 mM. (a) Bright-field microscopy images; (b) false-color images obtained by CARS microspectroscopy of glyceryl trioctanoate (red) and progesterone (green). The change in apparent color indicates the increasing predominance of progesterone with increasing time. (c) False-color images of the concentration of progesterone within the droplet (concentration given by color bar). Scale bar = $10\ \mu\text{m}$, pixel step size = $2\ \mu\text{m}$, 26×26 pixels, measurement time per image = 70 s. Enzyme concentration = $1.5\ \text{mg mL}^{-1}$. The color scale gives the progesterone concentration in panel c in mM.

Bright-field microscopy images of the digestion of a 95 mM progesterone solution in glyceryl trioctanoate over 90 min are shown in Figure 8a. No crystalline phase is observed during digestion, which suggests that the lipolytic products form structures smaller than the wavelength range of visible light. Such structures are expected to be micelles and vesicles.³⁹ Progesterone is also soluble in glyceryl trioctanoate at these concentrations, so the only visible change during digestion is that the droplet has shrunk. The concentration of the lipolytic products in the aqueous phase is below the detection limit of our experiment, so in Figure 8b, we show false-color CARS images of only the oil phase (red) and progesterone (green). We observe qualitatively that the drug remains homogeneously distributed throughout the drop and the concentration of the drug in the oil increases as the oil is digested. In order to quantify this concentration increase, we employ the calibration plot from Figure 7; images of the concentration of progesterone are shown in Figure 8c. Very similar results were observed for droplets containing Vitamin D₃.

We repeated this experiment for several droplets containing either progesterone or Vitamin D₃. The average concentration of Vitamin D₃ or progesterone in each droplet is plotted as a function of time in Figure 9a,c, respectively. The radius of each droplet is plotted as a function of time in Figure 9b,d, respectively. The results from a control experiment in which no enzyme was present in the aqueous phase are also plotted in Figure 9a,b.

For the control experiment, the radius of the droplet remained constant throughout the measurement but the average concentration of Vitamin D₃ in the droplet decreases over time. No digestion is occurring in this experiment, so no lipolytic products are present. Nonetheless, micelles of sodium taurodeoxycholate (bile salt micelles) are present in the aqueous phase, into which the drug can be solubilized. This mechanism lowers the concentration of Vitamin D₃ in the emulsion droplet.

For all of the other droplets, the concentration of the drug increases with time with a concomitant decrease in the droplet radius. The rate of change of the droplet radius obtained from the linear fits in Figure 9b,d, dr/dt , only varies from -0.05 to $-0.11\ \mu\text{m min}^{-1}$ for all four droplets. This relative lack of variation in dr/dt is surprising given that these droplets have different initial sizes and contain different additives at different concentrations. These observations suggest that, under these

(45) Fini, A.; Ospitali, F.; Zoppetti, G.; Puppini, N. *Pharm. Res.* **2008**, *25*, 2030–2040.

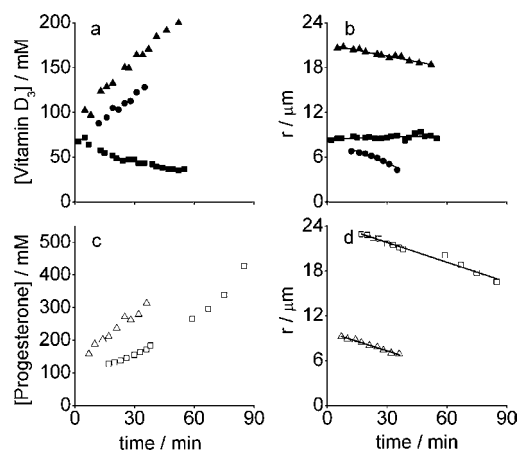


Figure 9. (a,c) Average drug concentration in glyceryl trioctanoate droplets during digestion by porcine pancreatic lipase plotted as a function of time. (b,d) Radius, r , of glyceryl trioctanoate droplets during digestion by porcine pancreatic lipase plotted as a function of time. Linear fits to the data are shown as solid lines. (a,b) Vitamin D₃, initial concentration = 75 mM. (c,d) Progesterone, initial concentration = 95 mM.

conditions, the rate of digestion is largely independent of the droplet size and the type of additive.

The increase in the concentration of the drug within the droplet is likely to be caused by the following mechanism. The enzyme hydrolyzes the triacylglyceride into lipolytic products, which form soluble colloidal structures, whence the decrease in the drop radius. The volume of the drop decreases, but the drug is more soluble in the oil phase than in the lipolytic products and hence the drug concentration increases. Nonetheless, our observations do not preclude some of the drug being solubilized by the lipolytic products, as noted in the control experiment. Ultimately, one would expect the drug to crystallize from these supersaturated solutions. Thus, from these results, we observe that, although these drugs have high solubilities in glyceryl trioctanoate, they have little solubility in the lipolytic products. Consequently, this simple excipient is not an optimal formulation for efficient drug delivery.

Conclusion

The digestion of lipids is a key factor in maintaining the health of the human body. The composition and rate of digestion of fatty meals are correlated to obesity, diabetes, and cardiovascular diseases. Digestion of lipids that contain oil-soluble nutraceuticals and vitamins directly influences the efficacy of these additives. Furthermore, the genesis of new diseases and syndromes, as well as the ability of pathogens to develop immunity to current drugs, will continue to drive the development of new pharmaceuticals. However, the potential of many of these new drugs will be lost or diminished without a thorough understanding of the mechanisms by which they are absorbed by the body. Here we have demonstrated the capability of multiplex CARS microspectroscopy to investigate lipid digestion, both in the presence and in the absence of oil-soluble additives.

We have shown that CARS can be used to discriminate between the undigested oil and the lipolytic products without labeling but based on their differing vibrational signatures alone. We note that spontaneous Raman microspectroscopy could also be used to study the digestion of lipids. However, CARS, as a coherent technique, has the advantage that stronger signals are obtained, which results in faster imaging. Indeed, the imaging

rates reported in this work are limited by the readout rate of the CCD camera not the signal level, so hardware improvements will lead to greater temporal resolution in the future. We also mapped the evolution of the digestion process in order to specify the locations at which the lipolytic products are generated. The phase of the lipolytic products is expected to affect the efficacy of an excipient as a drug delivery vehicle, and this expectation has stimulated numerous studies of phase behavior.^{6,11,39,46,47} Mixtures of oleic acid, glyceryl monooleate, and water exhibit cubic liquid crystal, oily liquid, and colloidal liquid phases. In this report, we did not discriminate between any potential variation in the local phase or composition of the lipolytic products. However, vibrational spectroscopy is, in principle, well-capable of discriminating phase polymorphism when the spectra of the pure phases are known.^{48,49} Thus, through the creation of representative mixtures of lipolytic products, it should prove possible to extend this concept to identify the spectra of the other phases that can be produced during digestion. This approach would allow a direct determination of the *local* composition and phase on the surface of an emulsion droplet during digestion, which would prove particularly useful when the excipient is not just a single triglyceride but a mixture of different lipids.

We have also shown that this technique is able to map the distribution of sterol crystals during digestion and to follow the dissolution of the crystals into the lipolytic products. We also observed that high local concentrations of the sterol affect the phase behavior of the lipolytic products. This observation is likely to be linked to the manner in which the lipid excipient affects the bioavailability of the sterol. We plan further experiments to probe this complex behavior further.

In this work, we have employed ergosterol as a model sterol as it offers a convenient spectral response. Nonetheless, these results point the way toward CARS microscopy of both phytosterols and cholesterol. The incorporation of phytosterols in food has been shown to lower blood cholesterol, but the detailed mechanism by which this occurs has not been elucidated. Digestion of the triacylglyceride carrier allows the sterol to be solubilized by dietary mixed micelles, from which the sterol is absorbed.⁵⁰ Phytosterols appear to limit the solubility of cholesterol in these micelles but may also cocrystallize with cholesterol within an oil drop during lipolysis; in both cases, the amount of cholesterol that can be absorbed is reduced.³³ Multiplex CARS microspectroscopy is suited to address this question, as cholesterol and phytosterols such as stigmasterol exhibit different spectral responses. From these responses, one could determine the concentration ratio of the sterols within oil droplets during the digestion process and hence whether these sterols are being competitively solubilized by dietary mixed micelles.

Finally, we mapped quantitatively the concentration of two representative lipophilic drugs, progesterone and Vitamin D₃, in emulsion droplets during digestion. The local concentration of Vitamin D₃ and progesterone within a droplet could be determined down to concentrations of ~ 5 and ~ 20 mM,

(46) Kossena, G. A.; Charman, W. N.; Boyd, B. J.; Porter, C. J. H. *J. Controlled Release* **2004**, *99*, 217–229.

(47) Nonomura, Y.; Nakayama, K.; Aoki, Y.; Fujimori, A. *J. Colloid Interface Sci.* **2009**, *339*, 222–229.

(48) Sprunt, J. C.; Jayasooriya, U. A.; Wilson, R. H. *Phys. Chem. Chem. Phys.* **2000**, *2*, 4299–4305.

(49) Da Silva, E.; Bresson, S.; Rousseau, D. *Chem. Phys. Lipids* **2009**, *157*, 113–119.

(50) Hui, D. Y.; Howles, P. N. *Semin. Cell Dev. Biol.* **2005**, *16*, 183–192.

respectively. Lower concentrations are feasibly accessible through the use of longer spectral integration times or through the use of electronic resonant enhancement for certain drugs.⁵¹ In the absence of enzyme, the concentration of Vitamin D₃ in an emulsion droplet decreased with time, which we ascribed to the solubility of this vitamin in the bile salt micelles present in the buffer solution. In the presence of enzyme, however, the drugs were found to concentrate within the emulsion droplet as the oil was hydrolyzed, which we have ascribed to their low solubility in the lipolytic products. These observations suggest that glyceryl trioctanoate is not an optimal formulation for efficient drug delivery for these drugs. Nevertheless, neither the type of drug nor the initial radius of the emulsion droplet had a large effect upon the rate of digestion under these conditions.

Although multiplex CARS microspectroscopy lacks the spatial resolution either to image a drug within a dietary mixed micelle directly or to determine the morphology of the liquid crystalline product phases on the nanometer length scale, it is evidently well-suited to follow the partitioning of a drug from the excipient into the lipolytic products without the need for labeling or invasive sample preparation. From these data, the partitioning of the drug into dietary mixed micelles can be inferred as the total number of drug molecules within the system is constant. Furthermore, CARS microscopy has already been shown to be readily suited to intracellular imaging,^{15,23,52–54} which suggests that CARS is also a promising and convenient technique to observe the absorption of fatty acids and drugs into intestinal cells.

Experimental Section

Sample Preparation. Porcine pancreatic lipase ([E.C. 3.1.1.3], activity ~ 20 U mg⁻¹) was obtained from Applchem Lifescience and used as received. Tris(hydroxymethyl)aminomethane (Tris), sodium chloride, calcium chloride, sodium azide, sodium taurodeoxycholate, glyceryl trioctanoate, glyceryl trioleate, ergosterol, Vitamin D₃, and progesterone were obtained from Sigma-Aldrich and used as received. The aqueous buffer phase consisted of 40 mM Tris, 150 mM NaCl, 8 mM CaCl₂, 13 mM sodium taurodeoxycholate, and 0.02% NaN₃ at pH 7.4; 1.5 mg mL⁻¹ enzyme solutions were created by dissolving the powdered enzyme in buffer solution, centrifuged to separate out any insoluble residue, and used immediately. Coarse oil-in-water emulsions were created by adding 5 wt % oil to buffer and sonicating. The digestion of oil droplets was initiated by mixing enzyme solution with the emulsion. An aliquot of this mixture was put between two glass coverslips separated by a 25 μ m PTFE spacer and placed into the multiplex CARS microscope. All experiments were performed at room temperature (~ 22 °C).

Multiplex CARS Microscope. CARS is a four-wave mixing process in which the CARS signal is emitted by a third-order polarization driven by a pump field, a Stokes field, and a probe field. The CARS signal is significantly enhanced when the frequency difference between the pump and Stokes fields coincides with a vibrational resonance of the sample, whence the chemical specificity. In multiplex CARS, the Stokes beam arises from a broad-band (femtosecond) laser and the pump and probe fields from the same narrow-band (picosecond) source. This arrangement allows the measurement of a broad portion of the vibrational spectrum (~ 400 cm⁻¹ spectral bandwidth) with high spectral resolution (~ 5 cm⁻¹). The experimental setup has been described in detail elsewhere.⁵⁵ The pump/probe (710 nm, 10 ps, 80 MHz) and Stokes (tunable from 750 to 950 nm, 80 fs, 80 MHz) beams from two Ti:sapphire lasers (Tsunami, Spectra-Physics) are overlapped in time and space and focused by a high NA oil-immersion microscope objective (40 \times , 1.30 NA) onto the sample. The spatial resolution of this CARS microscope has been shown to be 0.3 and 1 μ m in the lateral and axial directions, respectively.⁵⁶ The CARS signal is collected in the forward direction by an air-immersion objective (40 \times , 0.65 NA), optically filtered, dispersed by a spectrograph (Oriel, MS257), and the spectrum is acquired by a CCD camera (Andor, DV420). The sample itself is mounted on a piezo-driven stage (PZT P-611.3S, Physik Instrumente) and raster-scanned relative to the laser focus. Consequently a ~ 400 cm⁻¹ broad spectrum is acquired at each pixel of the raster scan. Hyperspectral CARS images were acquired with average pump and Stokes laser powers of 40 and 20 mW, respectively, and pixel dwell times of 20 ms.

Analysis of Spectra. The analysis of CARS spectra is complicated by the convolution of the vibrationally resonant term, with a nonresonant term arising from the electronic response of the material. Spectra of the imaginary part of the third-order nonlinear susceptibility, $\text{Im}[\chi^{(3)}]$, were retrieved from the raw CARS spectra by the maximum entropy method (MEM), as described elsewhere.⁵⁷ $\text{Im}[\chi^{(3)}]$ spectra are directly comparable to spontaneous Raman spectra, and the peak amplitudes or integrated intensities are proportional to the number of scatterers in the laser focus.

Acknowledgment. We thank Unilever R&D Vlaardingen and the SenterNovem Agency of the Dutch Ministry of Economic Affairs through the Food & Nutrition Delta 2 Program (Grant DFN0642300) for support of this work. K.F.D. thanks the Alexander von Humboldt Foundation (Germany) for a Feodor Lynen Fellowship. K.P.V. thanks Jack W. M. Seijen ten Hoorn and Elisabeth C. M. Bouwens for useful discussions. This work is part of the research program of the Stichting Fundamenteel Onderzoek der Materie (Foundation for Fundamental Research on Matter) with financial support from the Nederlandse Organisatie voor Wetenschappelijk Onderzoek (Netherlands Organization for the Advancement of Research).

JA102069D

(51) Min, W.; Lu, S.; Holtom, G. R.; Xie, X. S. *ChemPhysChem* **2008**, *10*, 344–347.

(52) Xie, X. S.; Yu, J.; Yang, W. Y. *Science* **2006**, 312.

(53) Le, T. T.; Cheng, J.-X. *PLoS ONE* **2009**, *4*, e5189.

(54) Kennedy, D. C.; Lyn, R. K.; Pezacki, J. P. *J. Am. Chem. Soc.* **2009**, *131*, 2444–2445.

(55) Muller, M.; Schins, J. M. *J. Phys. Chem. B* **2002**, *106*, 3715–3723.

(56) Wurpel, G. W. H.; Schins, J. M.; Muller, M. *Opt. Lett.* **2002**, *27*, 1093–1095.

(57) Vartiainen, E. M.; Rinia, H. A.; Muller, M.; Bonn, M. *Opt. Express* **2006**, *14*, 3622–3630.